Supporting information for

Deposition of a high entropy thin film by aerosol-assisted chemical vapor deposition

Weichen Xiao,[a] Mark A. Buckingham,[a] Yi Li,[a] Kerry Hazeldine,[b] Bing Han,[a] Sarah H. Cartmell,[a] Alexander S. Eggeman,[a] Alex S. Walton,[b] and David J. Lewis[a,*]

[a] Department of Materials, The University of Manchester, Manchester M13 9PL, UK

[b] Department of Chemistry and the Photon Science Institute, The University of Manchester, Oxford Road, Manchester, M13 9PL UK

* Corresponding author: david.lewis-4@manchester.ac.uk

Contents

Chemicals and Experimental

Chemicals: Sodium diethyldithiocarbamate trihydrate ($Na(S_2CNEt_2)$ 97%), copper(II) chloride ($CuCl_2$ 99%,), zinc (II) diethyldithiocarbamate ($Zn(S_2CNEt_2)_2$ 97%), cobalt chloride hexahydrate ($CoCl_2 \cdot 6H_2O$ 98%), gallium(III) nitrate ($Ga(NO_3)_3$ 99.9%), indium(III) chloride ($InCl_3$ 99.999%) were all purchased from Sigma Aldrich.

Instrumentation: Thermogravimetric analysis (TGA) was conducted under N_2 atmosphere from room temperature to 600 °C at a heating rate of 10 °C min^{-1} using a TGA STAR instrument (MettlerToledo). Infra-Red (IR) absorption spectroscopy was performed on a Brucker alpha Platinum ATR FTIR instrument. NMR spectroscopy was conducted on a Bruker, 400 MHz machine. Elemental analysis (EA) was performed using a Thermo Scientific Flash 2000 Organic Elemental Analyzer for CHN and S analyses. Mass spectrometry was performed using Thermo Q Exactive hesi POS instrument. The crystal structure of synthesised HES was examined by powder X-ray diffraction (p-XRD) using a Bruker D8 Discover diffractometer with Cu Kα radiation (λ = 0.15418 nm). XRD data was collected using a line X-ray source with a width of 16 mm, which covers the whole film (with a width of 15 mm and a length of 20 mm). Thus, the data is an average over the whole film. The morphology and elemental distribution of the HES was investigated by FEI Quanta 650 SEM operating at 20 kV and 200 keV FEI Talos F200A for the TEM. Raman spectroscopy was performed on a Horiba LabRAM instrument using a 488 nm wavelength laser at 10% power. Optical measurements were recorded on a Shimadzu UV-1800 in the wavelength range of 1100−300 nm.

XPS: The HAXPES instrument at the University of Manchester, in which both the XPS and HAXPES were conducted sequentially within the same run, consists of a Ga Kα1 X-ray source (hv = 9251.7 eV) with a bespoke monochromator, monochromated Al Kα X-ray source (hv = 1486.6 eV), and a EW4000 electron energy analyser. All the XPS and HAXPES core level spectra were fitted using CasaXPS peak fitting software using a Voigt function and generally a Shirley background type was used. From the XPS and HAXPES survey spectra (Figures S19 and S20), the atomic percentage composition of the HEMS thin films can be calculated, as shown in Tables S5 and S8. The atomic percentage composition was determined using CasaXPS peak fitting software and the appropriate relative sensitivity factors (RSF). All XPS and HAXPES spectra was charged referenced to the metal sulfide peak in the S 2p at 161.7 eV. Due to the composition of the material, adventitious carbon and metallic peaks cannot be used as suitable binding energy references, therefore the lattice sulfur was used in a similar approach to lattice oxygen binding energy charge referencing in metal oxides.[1]

Precursor synthesis: $Cu(DTC)_2$ was synthesised following a literature procedure,[2] briefly: sodium diethydithiocarbamate trihydrate (1.80 g, 8 mmol) was dissolved in methanol (30 ml). Copper chloride (0.54 g, 4 mmol) was dissolved in a separate solution of methanol (20 mL). The solution of copper chloride was added dropwise to the diethyldithiocarbamate solution. Once fully added, the mixture was stirred for 1 h at room temperature. The resulting precipitate was then collected by vacuum filtration, washed with methanol and DI water at room temperature and dried under vacuum overnight. The final product was a dark brown solid (yield 85.8%). $In(DTC)_3$ and $Ga(DTC)_3$ were synthesised using the same method as $Cu(DTC)_2$, with the exception that indium chloride (0.88g, 4 mmol) and gallium nitrate (1.04g, 4 mmol) were the sources of indium and gallium. These syntheses required a 3 : 1, DTC : metal ratio with sodium diethydithiocarbamate trihydrate (2.71g, 12 mmol) used. The final products were white solids (yields of $In(DTC)_3$ 81.1%; $Ga(DTC)_3$ 76.9%). $Co(DTC)_3$ was synthesised using the same method as $Cu(DTC)_2$, where cobalt chloride hexahydrate (0.95g 4 mmol) was the cobalt source. A higher amount of sodium diethydithiocarbamate trihydrate (2.71g, 12 mmol) was required as the Co(II) oxidises to Co(III). This reaction required a further purification step. The initial, crude product (collected after initial vacuum filtration) was dissolved in 20 ml of dichloromethane and stirred for 5 mins, to this solution, 10 mL of ethanol was added and stirred for a further 5 mins. The stirring was stopped and allowed to rest for a further 5 mins to allow precipitation of pure product, which was collected by vacuum filtration, which yielded a dark green solid (yield 60.7%).

Precursor analysis:

$Cu(DTC)_2$: Elemental analysis found (calculated) for $CuC_{10}H_{20}N_2S_4$ (%): C 33.36 (33.36), H 5.49 (5.60), N 7.74 (7.78), S 35.73 (35.62). FTIR ν_{max} (cm^{-1}): 2870, 2929, 2981. MS-ES m/z: 358.98. Melt point (°C): 198

$Co(DTC)_3$ $\cdot H_2O$: Elemental analysis found (calculated) for $CoC_{15}H_{30}N_3S_6\cdot H_2O$ (%): C 34.8 (34.50), H 5.96 (5.75), N 7.96 (8.05), S 36.92 (36.80). FTIR ν_{max} (cm^{-1}): 2868, 2927, 2973. MS-ES m/z: 354.98. Melt point (°C): 262

$Zn(DTC)_2$: Elemental analysis found (calculated) for $ZnC_{10}H_{20}N_2S_4$ (%): C 33.48 (33.19), H 5.47 (5.57), N 7.80 (7.74), S 35.38 (35.42), Zn 18.07 (17.87). ^1H NMR (400 MHz, DMSO): δ 3.81 (q, 4 H), 1.28 (t, 6 H). FTIR ν_{max} (cm^{-1}): 2871, 2928, 2966, 2979. MS-ES m/z (+Na): 382.97. Melt point (°C): 179

$In(DTC)_3$: Elemental analysis found (calculated) for $InC_{15}H_{30}N_3S_6$ (%): C 32.50 (32.20), H 5.31 (5.40), N 7.61 (7.51), S 35.47 (34.36), In 20.11 (20.52). ^1H NMR (400 MHz, DMSO): δ 3.78 (q, 4 H), 1.25 (t, 6 H). FTIR ν_{max} (cm^{-1}) :2868, 2926, 2972 MS-ES m/z (+Na): 581.97. Melt point (°C): 257

$Ga(DTC)_3$ $\cdot H_2O$: Elemental analysis found (calculated) for $GaC_{15}H_{30}N_3S_6\cdot H_2O$ (%): C 33.90 (33.83), H 5.62 (6.06), N 7.93 (7.89), S 35.76 (36.12). ^1H NMR (400 MHz, DMSO): δ 3.72 (q, 4 H), 1.22 (t, 6 H). FTIR ν_{max} (cm^{-1}): 2867, 2927, 2974. MS-ES m/z: 514.94. Melt point (°C): 246

AACVD: The setup of a typical AACVD process is shown in Fig S1. 0.1 mmol of each precursor ($Cu(DTC)_2$, $Co(DTC)_3$, $Zn(DTC)_2$, $Ga(DTC)_3$, $In(DTC)_3$) was combined and dissolved in 10 mL of tetrahydrofuran. The resulting combined precursor solution was transferred to a two-neck round bottom flask and placed above the aerosol generator. One of the necks of the round bottom flask was connected to an inlet of Ar gas at 200 cm^3 min^{-1}. Separately, glass substrates of size 20 × 15 mm were added to a glass reaction vessel and placed into a tube furnace. The second neck of the round bottom flask containing precursor solution was then connected to the inlet of the glass reaction vessel containing the glass substrates. This system was allowed to stand and come to an Ar atmosphere for 30 mins. After this time the oven was switched on and allowed to equilibrate at 550 °C. Once the oven reached the desired temperature the aerosol generator was switched on and the AACVD deposition allowed to occur for 1 h. After this time the oven was switched off and allowed to cool before the black substrates were collected. The substrates were placed at the beginning of the furnace and measurements of the furnace temperature at this position was lower than that of the set furnace temperature (340°C – 428°C *vs* 550°C). This was done as the decomposition of precursors occurred in this region of the furnace. TGA profiles of the precursors shows that they all decompose by *ca.* 375°C.

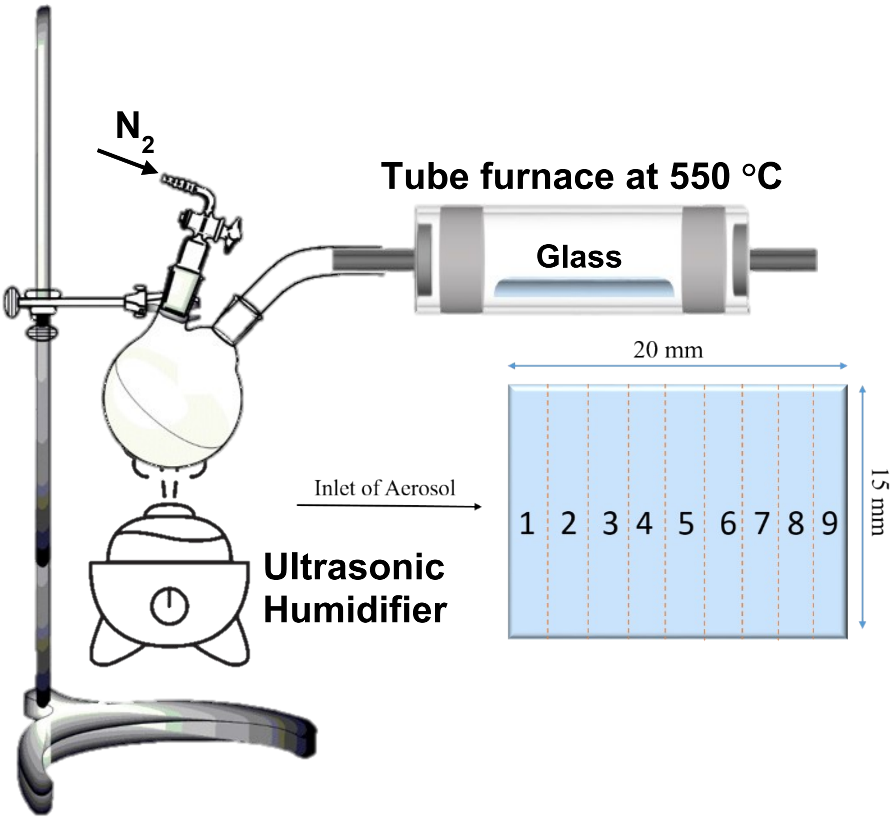

Figure S1. A typical AACVD setup and substrate details.

Calculation of configurational entropy ΔS_{conf}: The ΔS_{conf} was calculated using the at.% determined from the SEM-EDX analysis in Figures S10 – S18 and the equation below that takes into account HE materials with multiple sub-lattices. [3, 4]

$$\Delta S_{conf} = -R\sum_{S} a^{S} \sum_{i} y_i^{S} ln y_i^{S}$$

Precursor characterisation

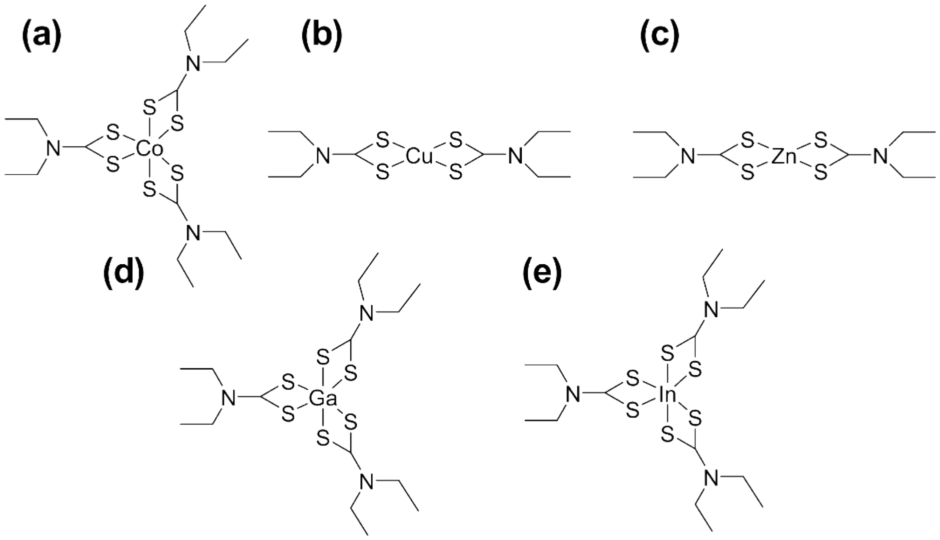

Figure S2. Chemical structures of the five synthesised diethyldithiocarbamate single source precursors (a) Co(DTC)$_3$, (b) Cu(DTC)$_2$, Zn(DTC)$_2$, Ga(DTC)$_3$, In(DTC)$_3$.

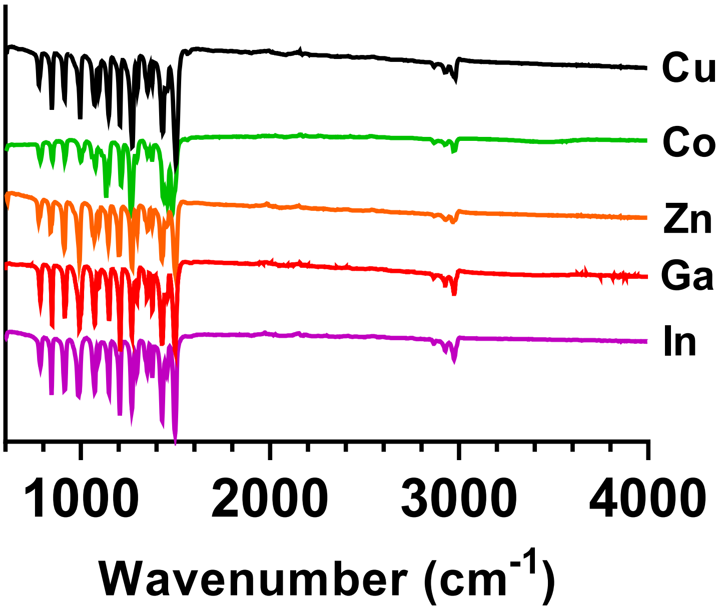

Figure S3. Structures of metal diethyl dithiocarbamate precursors.

Thermal decomposition of precursors

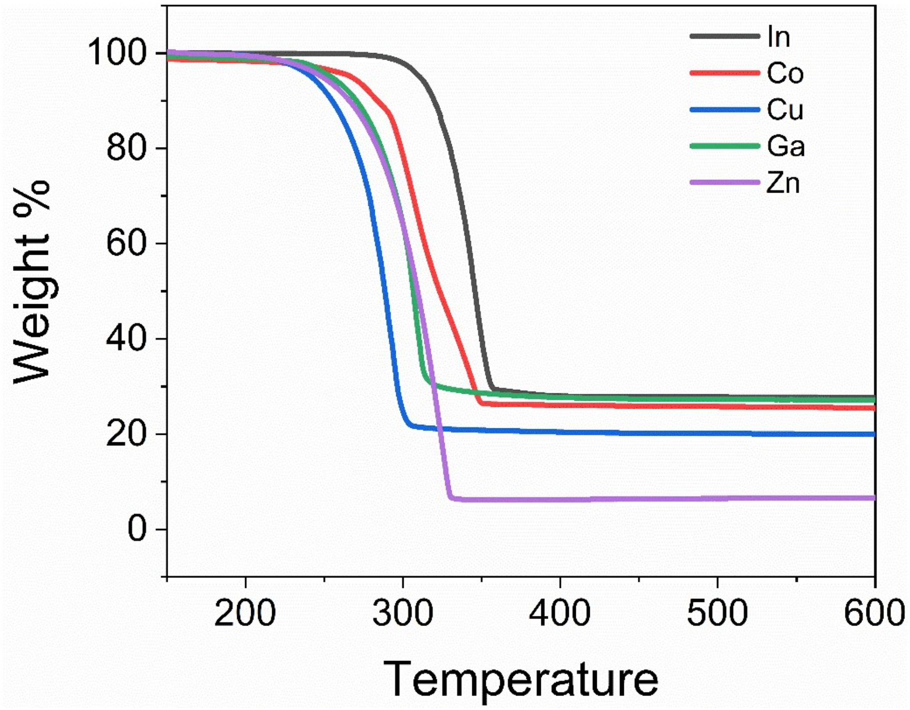

Figure S4. Thermogravimetric (TGA) of all precursors used.

Table S1. Decomposition windows of precursors.

Precursor	Onset T / °C	50% decomposition T / °C	End T / °C	Range / °C
In	310	338	358	48
Co	266	312	350	84
Cu	241	284	305	64
Ga	254	299	320	66
Zn	248	309	330	82

Powder X-ray diffraction (pXRD) of deposited (CoCuZnInGa)S

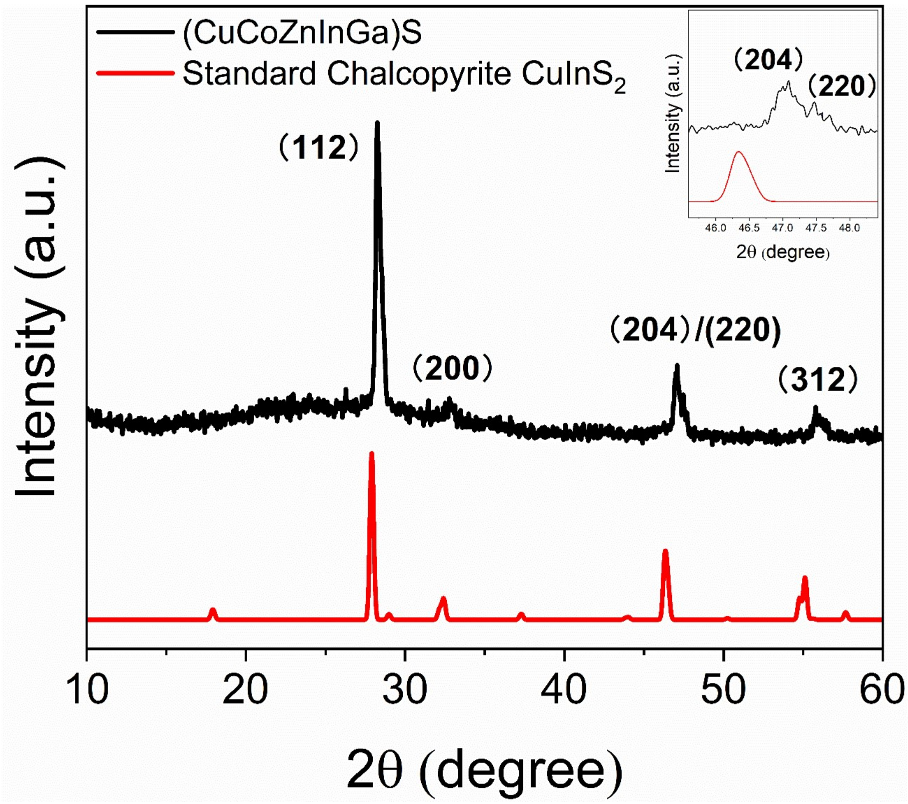

Figure S5. Grazing incidence x-ray diffraction (GIXRD) pattern of deposited film and a standard chalcopyrite film (CuInS$_2$, ICSD: 66865) reference.

Crystal lattice of the HE chalcopyrite structure

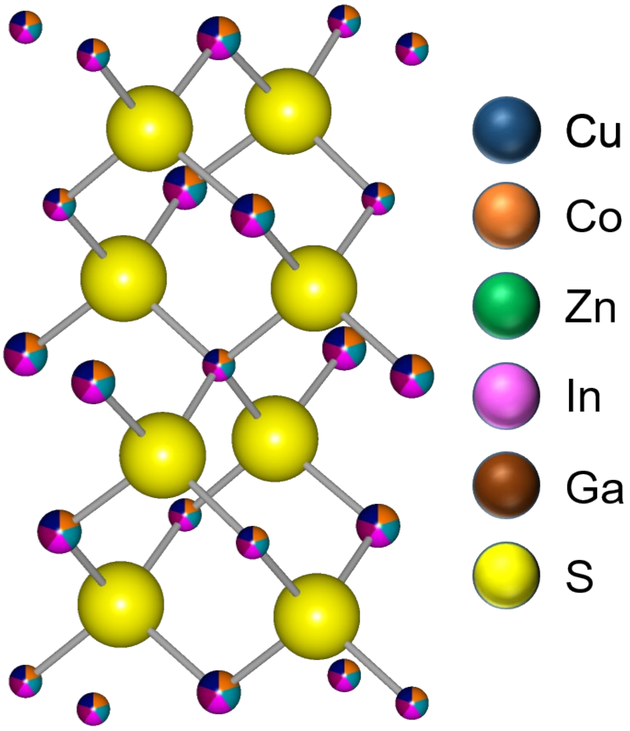

Figure S6. Structural model of synthesised materials, a = b = 5.52279(7), c = 11.13295(22), α = β = γ = 90°, space group: $I\bar{4}2d$, (ICSD: 66865).

Rietveld refinement

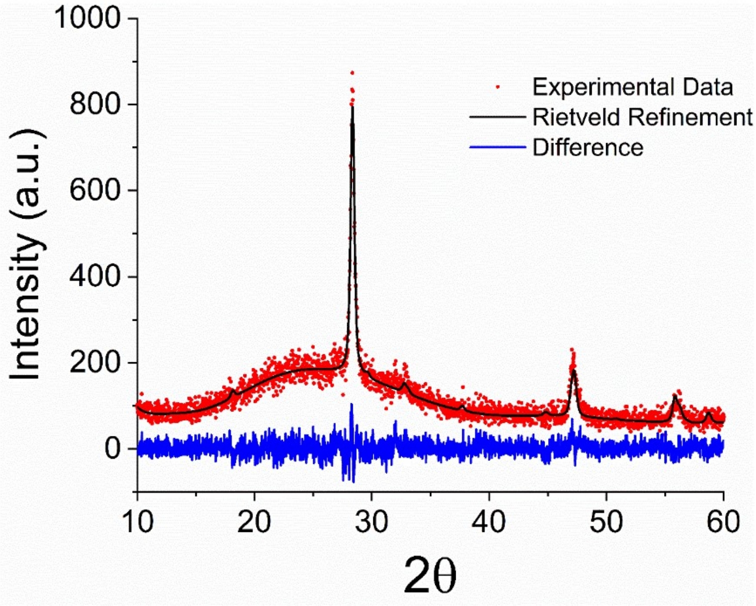

Figure S7. Rietveld Refinement of XRD data

Table S2. Refined lattice parameters, R values and goodness of fitting

Parameters	**$CuInS_2$ (ICSD: 66865)**	**Refined XRD**
a = b (Å)	5.54	5.47
c (Å)	11.09	10.82
Rep	/	9.40
Rwp	/	13.86
GOF	/	1.47

Table S3. Shannon prewitt crystal radii for elements in HEMS thin film.[5]

Element	**Ionic radii (Å)**
Cu (I)	0.74
Zn (II)	0.74
Co (III)	0.69
In (III)	0.76
Ga (III)	0.61

Selected Area Electron Diffraction

Powders were scraped off from the whole film and ground between 2 glass slides. The ground powders were then transferred to an Au carbon supported TEM sample grid. Five SAED patterns (Fig. S8 (a-e)) from different areas were taken and compared. All areas yielded identical azimuthal integrals which are compiled in Fig. S8(f), confirming the monophasic nature of the material. The diffraction patterns were also indexed to the $CuInS_2$ chalcopyrite structure. The *d* spacings measured are therefore consistent with the bulk pXRD results. The spikes from the main beam are due to an over saturated beam on the detector. This affected the brightness and is the reason for the contrast difference between images.

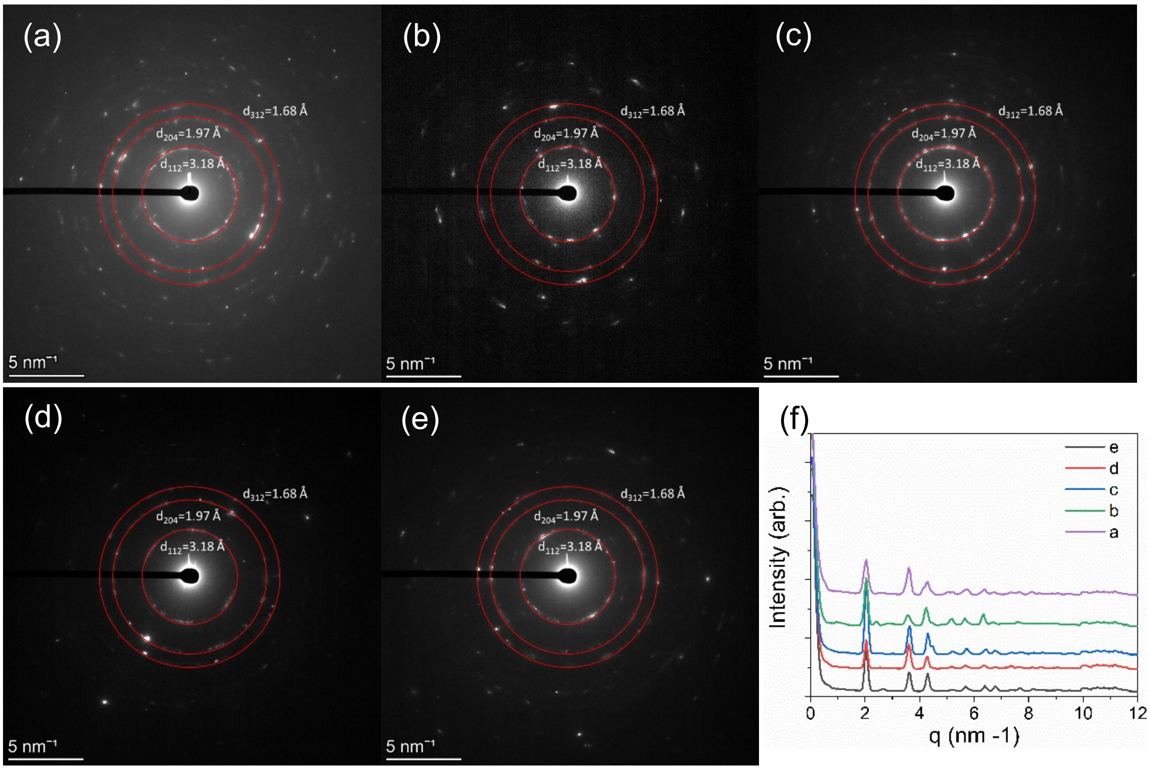

Figure S8. (a – e) 5 selected area electron diffraction (SAED) patterns from all areas of the (MoCoCuInGa)S thin film and (f) the azimuthal integrals of the 5 SAED patterns.

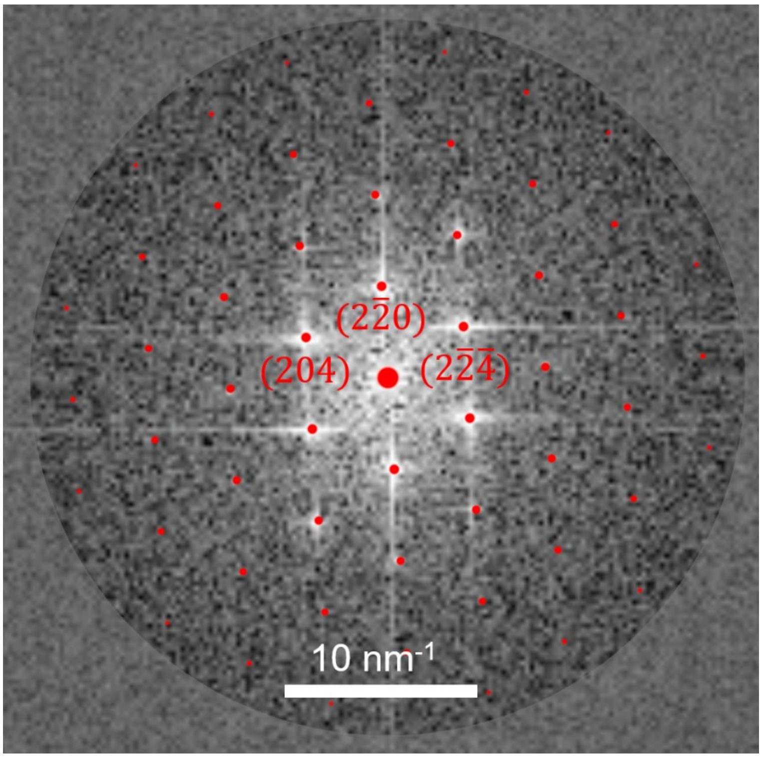

Figure S9. FFT from Figure 1(a) in the main text, overlayed with a $CuInS_2$ diffraction pattern simulated by Single Crystal in a (22-1) direction.

Scanning electron microscopy (SEM)

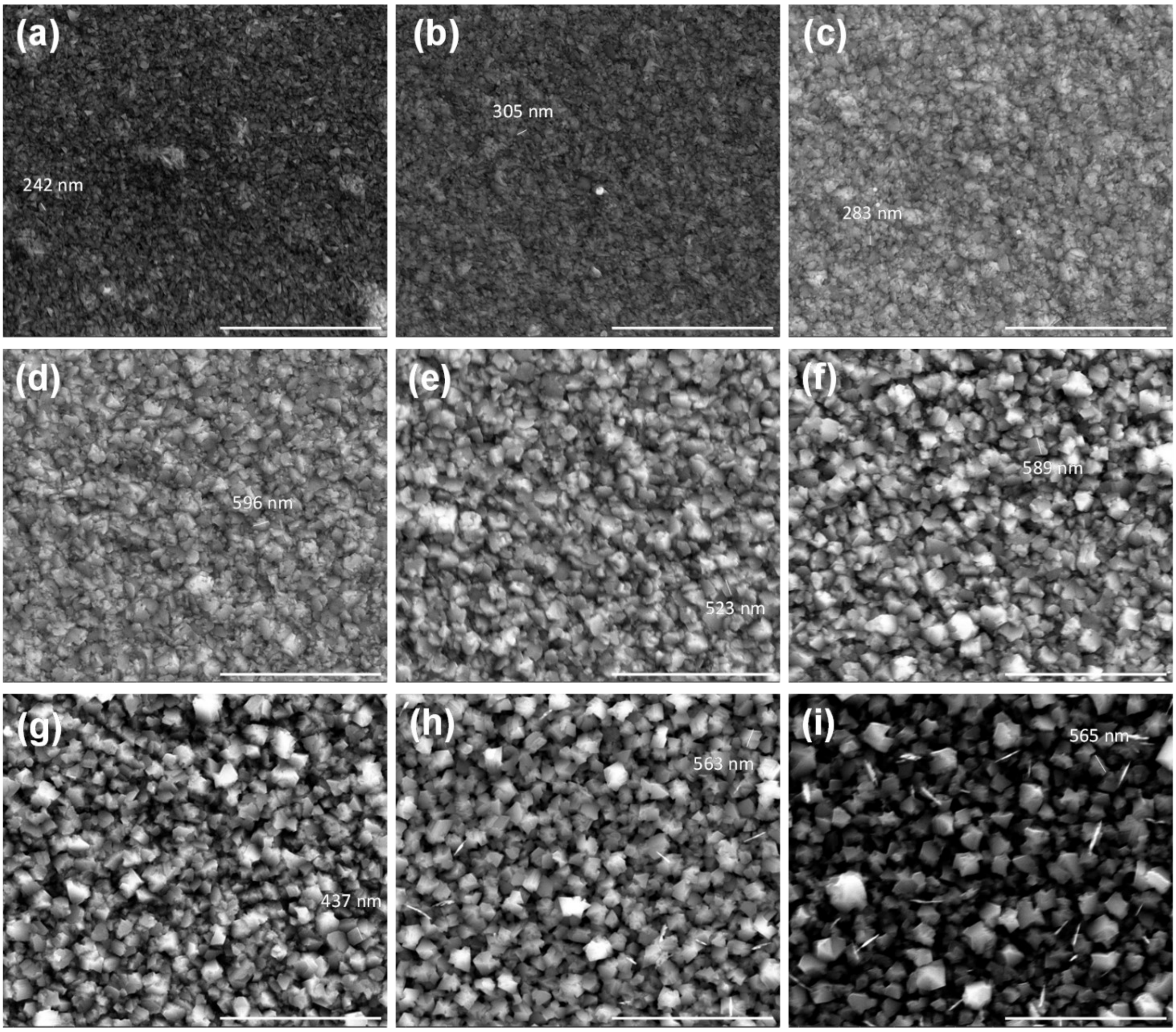

Figure S10. Change of crystal size and morphology from position (a) 1 (0.0 – 2.2 mm), (b) 2 (2.3 – 4.5 mm), (c) 3 (4.6 – 6.8 mm), (d) 4 (6.9 – 9.1 mm), (e) 5 (9.3 – 11.5 mm), (f) 6 (11.6 – 13.7 mm), (g) 7 (13.8 – 16.0 mm), (h) 8 (16.1 – 18.3 mm), (i) 9 (18.4 – 20.0 mm) of the deposited film. All scale bars in the graph are 5 μm.

Table S4. Table of data from particle size analysis of SEM images in Figure S9.

Position (distance mm)	Average particle size / nm
1 (0.0 – 2.2)	272 ± 72
2 (2.3 – 4.5)	279 ± 87
3 (4.6 – 6.8)	329 ± 99
4 (6.9 – 9.1)	494 ± 107
5 (9.3 – 11.5)	489 ± 128
6 (11.6 – 13.7)	555 ± 132
7 (13.8 – 16.0)	524 ± 127
8 (16.1 – 18.3)	538 ± 103
9 (18.4 – 20.0)	599 ± 154

SEM-EDX maps

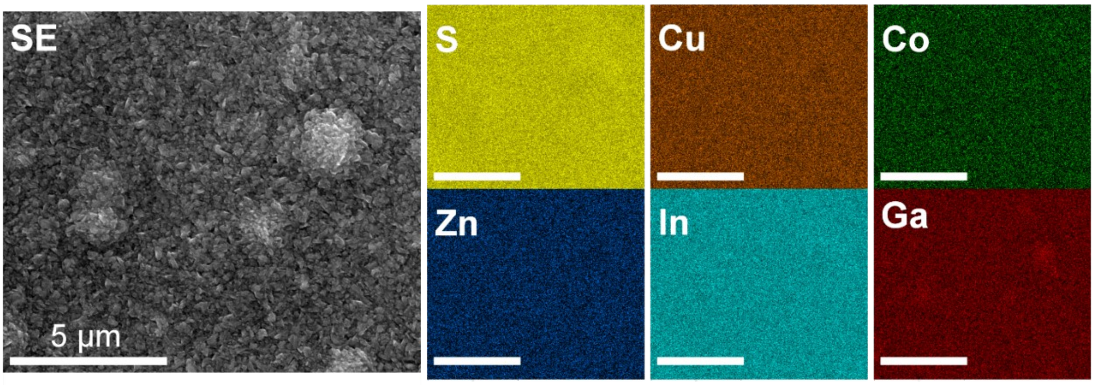

Figure S11. SEM-EDX mapping of position 1 (*ca.* 0.0 – 2.2 mm), with a 20 keV accelerating voltage. At.% Cu (17.6%), Co (1.1%), Zn (4.3%), Ga (13.8%), In (16.9%), S (46.3%).

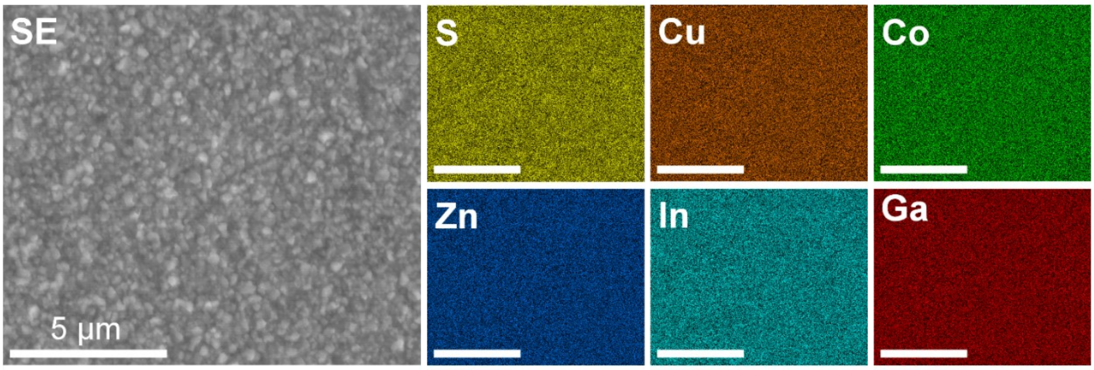

Figure S12. SEM-EDX mapping of position 2 (*ca.* 2.3 – 4.5 mm), with a 20 keV accelerating voltage. At.% Cu (16.8%), Co (2.8%), Zn (8.9%), Ga (8.0%), In (15.4%), S (48.0%).

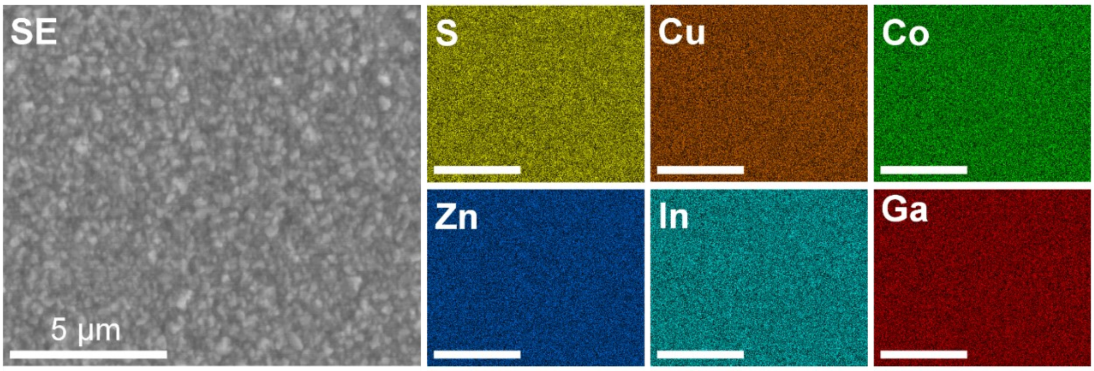

Figure S13. SEM-EDX mapping of position 3 (*ca.* 4.6 – 6.8 mm), with a 20 keV accelerating voltage. At.% Cu (15.9%), Co (3.6%), Zn (10.7%), Ga (6.8%), In (14.5%), S (48.5%).

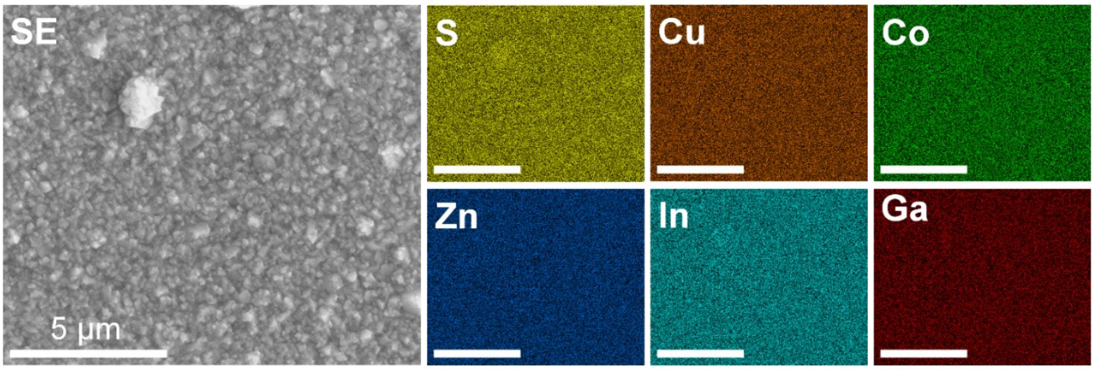

Figure S14. SEM-EDX mapping of position 4 (*ca.* 6.9 – 9.1 mm), with a 20 keV accelerating voltage. At.% Cu (14.5%), Co (5.3%), Zn (12.7%), Ga (5.1%), In (13.3%), S (49.2%).

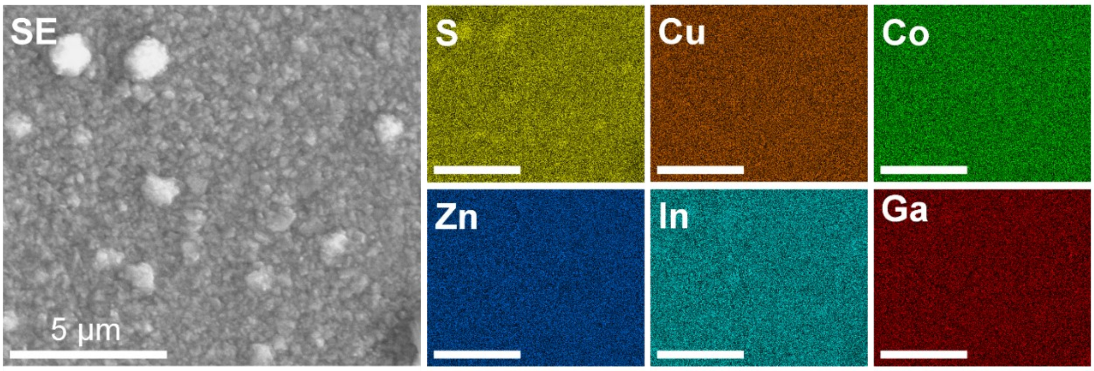

Figure S15. SEM-EDX mapping of position 5 (*ca.* 9.2 – 11.4 mm), with a 20 keV accelerating voltage. At.% Cu (13.2%), Co (7.3%), Zn (13.6%), Ga (3.7%), In (12.3%), S (49.8%).

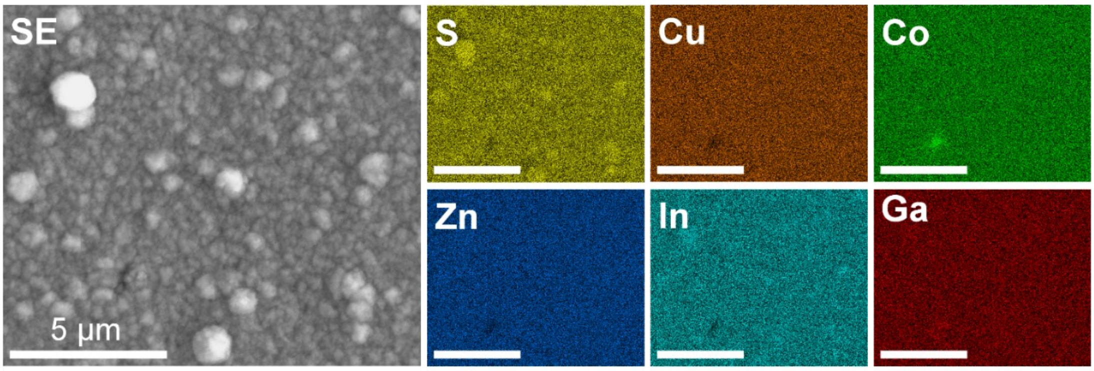

Figure S16. SEM-EDX mapping of position 6 (*ca.* 11.5 – 13.7 mm), with a 20 keV accelerating voltage. At.% Cu (11.9%), Co (9.7%), Zn (13.8%), Ga (2.4%), In (11.6%), S (50.7%).

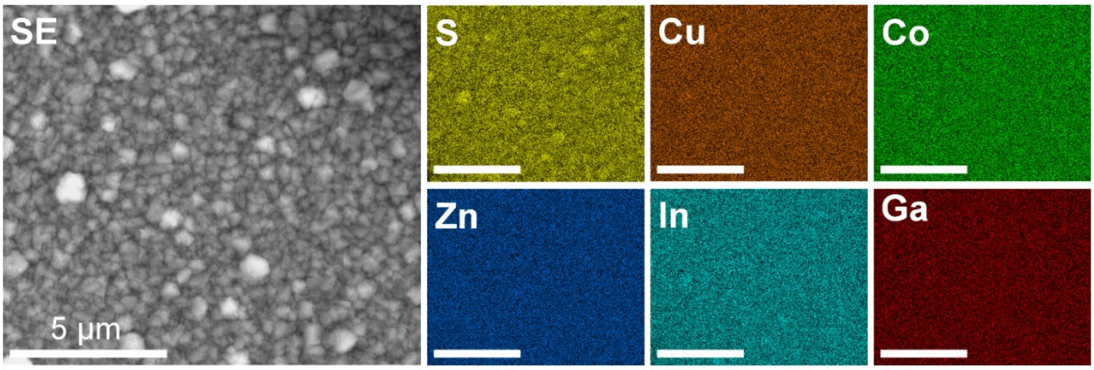

Figure S17. SEM-EDX mapping of position 7 (*ca.* 13.8 – 16.0 mm), with a 20 keV accelerating voltage. At.% Cu (11.0%), Co (11.1%), Zn (14.2%), Ga (1.4%), In (11.2%), S (50.9%).

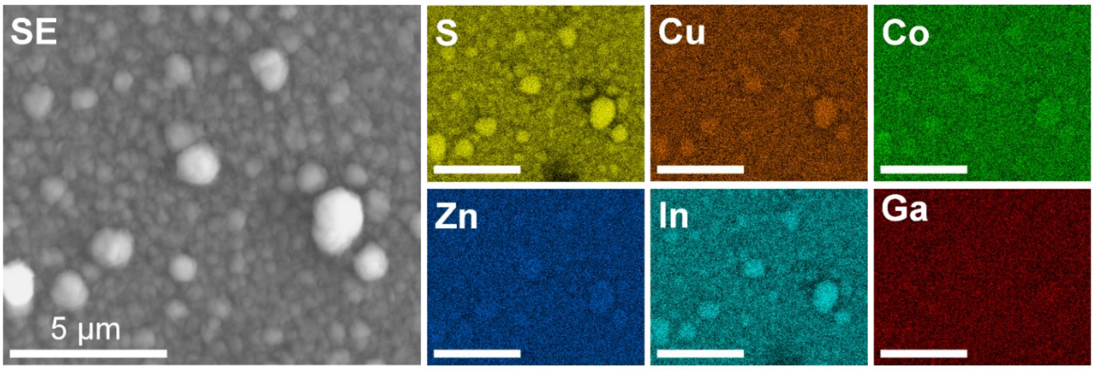

Figure S18. SEM-EDX mapping of position 8 (*ca.* 16.1 – 18.0 mm), with a 20 keV accelerating voltage. At.% Cu (10.1%), Co (12.8%), Zn (14.7%), Ga (0.8%), In (10.9%), S (50.7%).

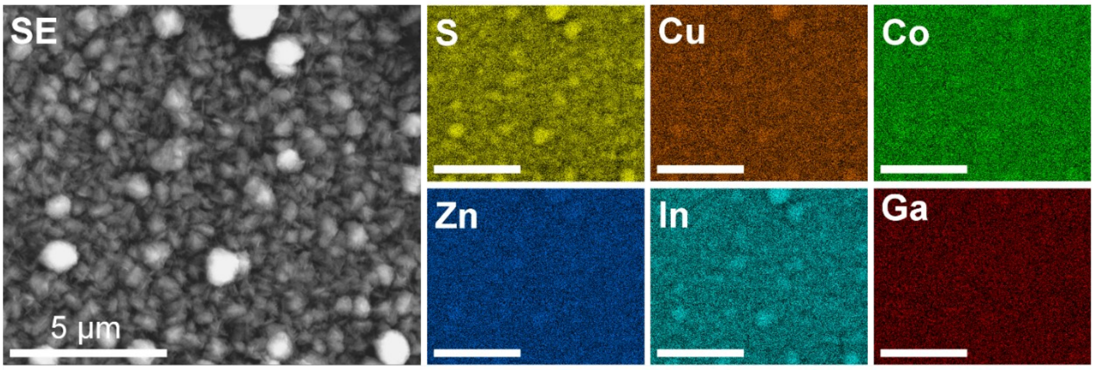

Figure S19. SEM-EDX mapping of position 9 (*ca.* 18.1 – 20.0 mm), with a 20 keV accelerating voltage. At.% Cu (8.9%), Co (13.8%), Zn (15.5%), Ga (0.5%), In (10.5%), S (50.8%).

Table of Data for Element across film±

Table S5. Table of data for elemental composition across the (CuCoZnInGa)S high entropy metal sulfide thin film in Figure 3(b).

Position (distance mm)	Cu / %	Co / %	Zn / %	In / %	Ga / %
1 (0.0 – 2.2)	17.8 ± 0.5	1.0 ± 0.3	5.7 ± 1.3	15.7 ± 1.9	12.6 ± 2.3
2 (2.3 – 4.5)	17.5 ± 0.6	2.0 ± 0.8	8.1 ± 0.8	14.4 ± 2.8	9.7 ± 2.6
3 (4.6 – 6.8)	16.4 ± 0.9	2.8 ± 1.3	10.5 ± 1.0	13.5 ± 2.3	8.2 ± 2.6
4 (6.9 – 9.1)	15.1 ± 1.4	4.1 ± 1.4	13.1 ± 1.6	11.9 ± 1.5	6.5 ± 1.9
5 (9.3 – 11.5)	14.1 ± 1.3	5.5 ± 1.7	14.3 ± 1.4	11.2 ± 1.5	5.2 ± 1.8
6 (11.6 – 13.7)	13.2 ± 1.3	7.5 ± 2.0	14.9 ± 1.0	10.4 ± 1.3	3.9 ± 1.4
7 (13.8 – 16.0)	12.6 ± 1.2	9.4 ± 1.3	15.1 ± 1.2	10.1 ± 1.7	2.3 ± 0.7
8 (16.1 – 18.3)	11.7 ± 1.4	11.8 ± 0.7	15.2 ± 1.1	9.6 ± 1.6	1.0 ± 0.5
9 (18.4 – 20.0)	9.6 ± 1.5	13.5 ± 1.3	16.1 ± 1.3	9.2 ± 1.7	0.7 ± 0.3

Raman spectroscopy of (CoCuZnInGa)S

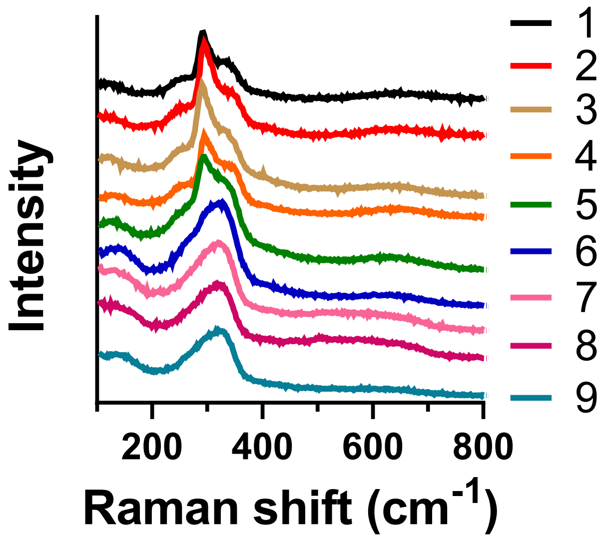

Figure S20. Raman spectrum of the film from 100 – 800 cm^{-1} range.

X-ray photoelectron spectroscopy (XPS)

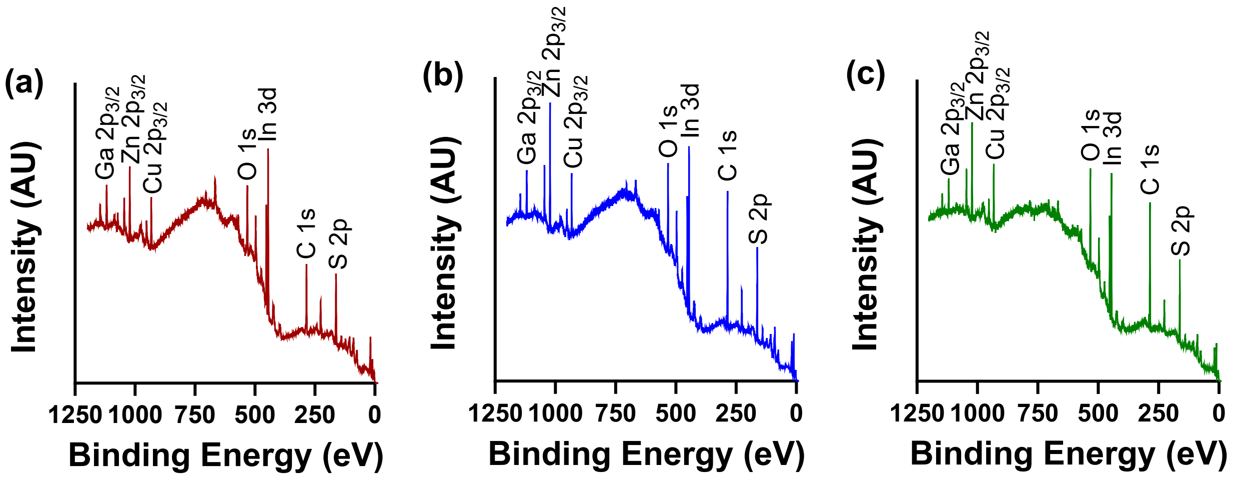

Figure S21. Survey spectra from XPS from (a) position 1 (initial 4 mm), (b) between 8 – 12 mm and (c) between 16 – 20 mm.

Table S6. Table of data from XPS atomic% analysis (including C and O).

XPS	Position		
	1	**5**	**9**
C	44.2	55.0	55.9
O	15.9	14.0	15.4
Co	0.0	0.0	1.0
Cu	1.8	1.2	1.3
Zn	2.4	2.4	1.9
Ga	1.4	1.0	0.8
In	6.5	3.9	3.1
S	27.8	22.4	20.5

Table S7. Table of data from XPS atomic% analysis (excluding C and O).

XPS	Position		
	1	**5**	**9**
Co	0.0	0.0	3.5
Cu	4.5	3.9	4.5
Zn	6.0	7.8	6.6
Ga	3.5	3.2	2.8
In	16.3	12.6	10.8
S	69.7	72.5	71.7

Hard X-ray photoelectron spectroscopy (HAXPES)

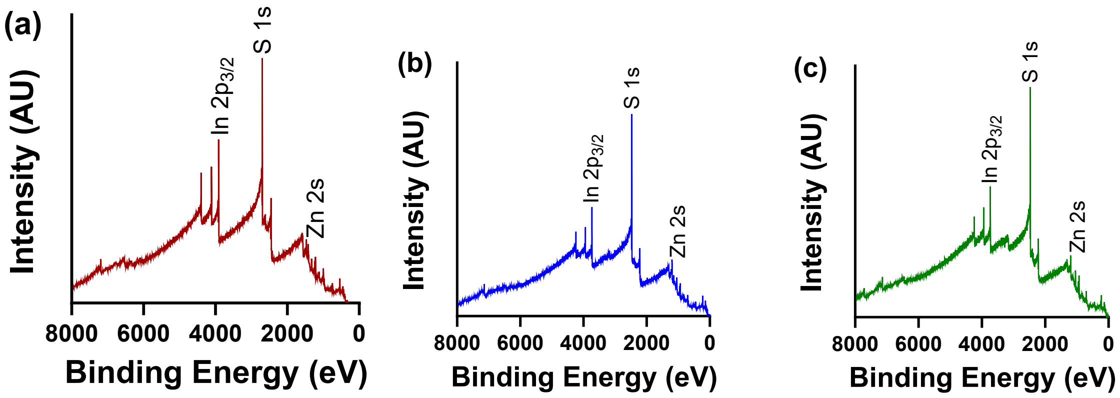

Figure S22. Survey spectra from HAXPES from (a) position 1 (initial 4 mm), (b) between 8 – 12 mm and (c) between 16 – 20 mm.

Sulfur core level fitting

Due to the high photon energy of HAXPES, both the S 1s and the S 2p core level spectra can be acquired, with the relative sensitivity factor (RSF) of S 1s being much greater than S 2p and thus demonstrating significantly better signal to noise.

The binding energy of the main peak in the S 1s spectra (Figure S21 (a – c) of the HEMS is at ~ 2469.7 to 2470.3 eV and is attributed to metal sulfide, which is consistent with the binding energy position 1617. eV in the S 2p (Figures S21 (d – f). The S 2p sulfide peak is fitted with a doublet with a spin orbit splitting of 1.16 eV. At measurement positions between 16 mm and 20 mm, an additional peak is observed in the S 1s at 2471.5 eV which is attributed to a further sulfide environment. In the S 2p spectra of all measurement positions, an additional broad peak at a lower binding energy ~ between 159 and 160 eV is observed and is attributed to the overlapping of the Ga 3s peak (indicated in Fig. S21(d) in green).

Table S8. The binding energy positions of the S 1s, Zn $2p_{3/2}$, In $3d_{5/2}$, Ga $2p_{3/2}$, and Cu $2p_{3/2}$ across the different positions of the film. The binding energy shift across the positions is consistent across all the core level spectra suggesting that this shift is a result of different charge regions within the film.

Binding Energy	S 1s	Zn $2p_{3/2}$	In $3d_{5/2}$	Ga $2p_{3/2}$	Cu $2p_{3/2}$
Position 1	2470.3	1022.6	445.3	1118.7	932.7
Position 5	2469.9	1022.2	444.9	1118.4	932.3
Position 9	2469.7	1022.0	444.8	1118.3	932.1

The peak associated with the metal sulfate is typically observed at ~2478 – 2479 eV in the S 1s and 168 – 169 eV in the S 2p. As shown in Figure S21, a peak associated with a metal sulfate is not observed in these spectra, and therefore the sulfate observed in the XPS is thought to just be present on the surface.

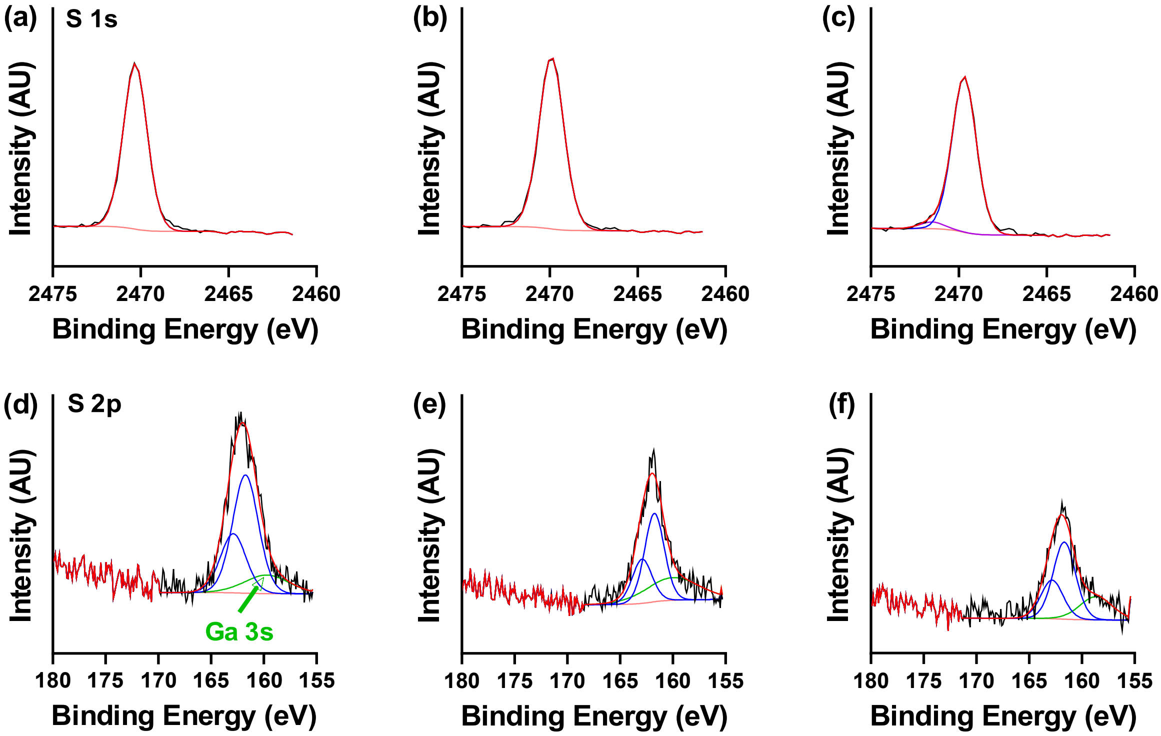

Figure S23. Figure showing fitting for HAXPES (a – c) S 1s core level and (d – f) S 2p measured from (a, d) position 1 (initial 4 mm), (b, e) between 8 – 12 mm and (c, f) between 16 – 20 mm.

Metal core level fitting

In all the high-resolution core level spectra of the metals in the HEMS except cobalt, a single doublet peak can be fitted, as shown in Figure S22. The doublets in all the metal core level spectra exhibit a symmetric line shape which is indicative of the component being a non-metallic chemical species.

The binding energy of the peaks in all the core level spectra (Table S7) are consistent with literature for the metal sulfide. There is no trace of a metal sulfate or oxidised metal in the core level spectra in Figure S22 which is typically observed at a higher binding energy.

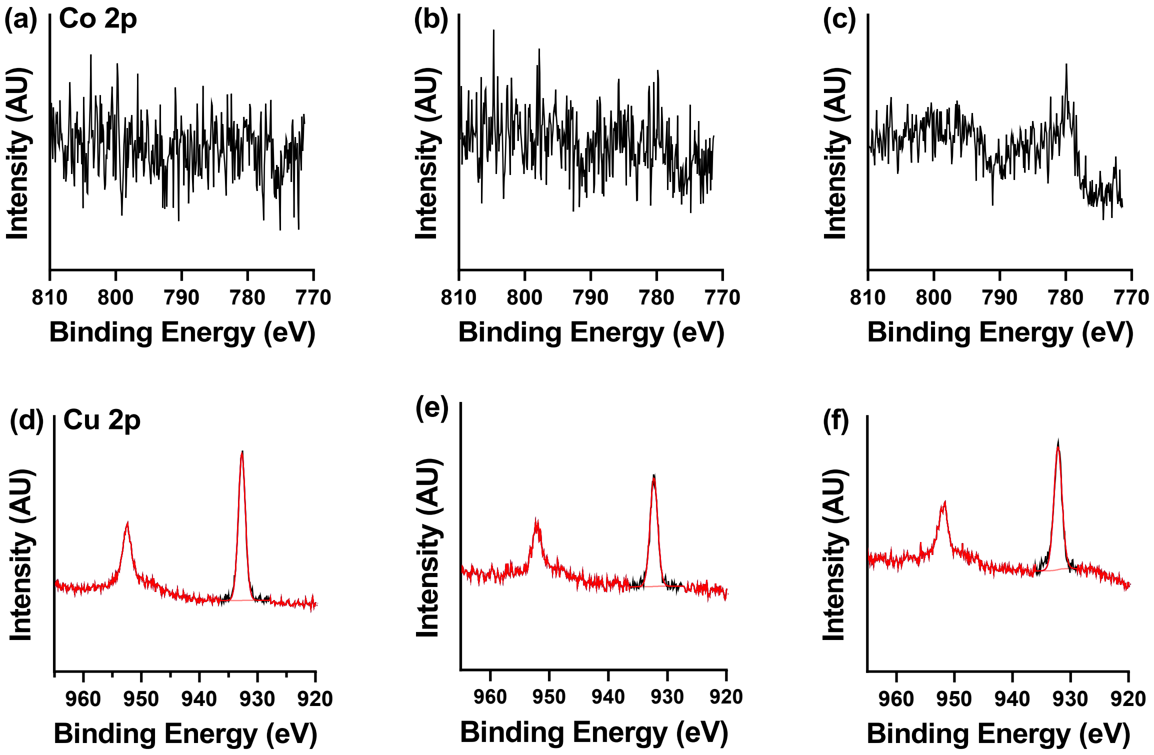

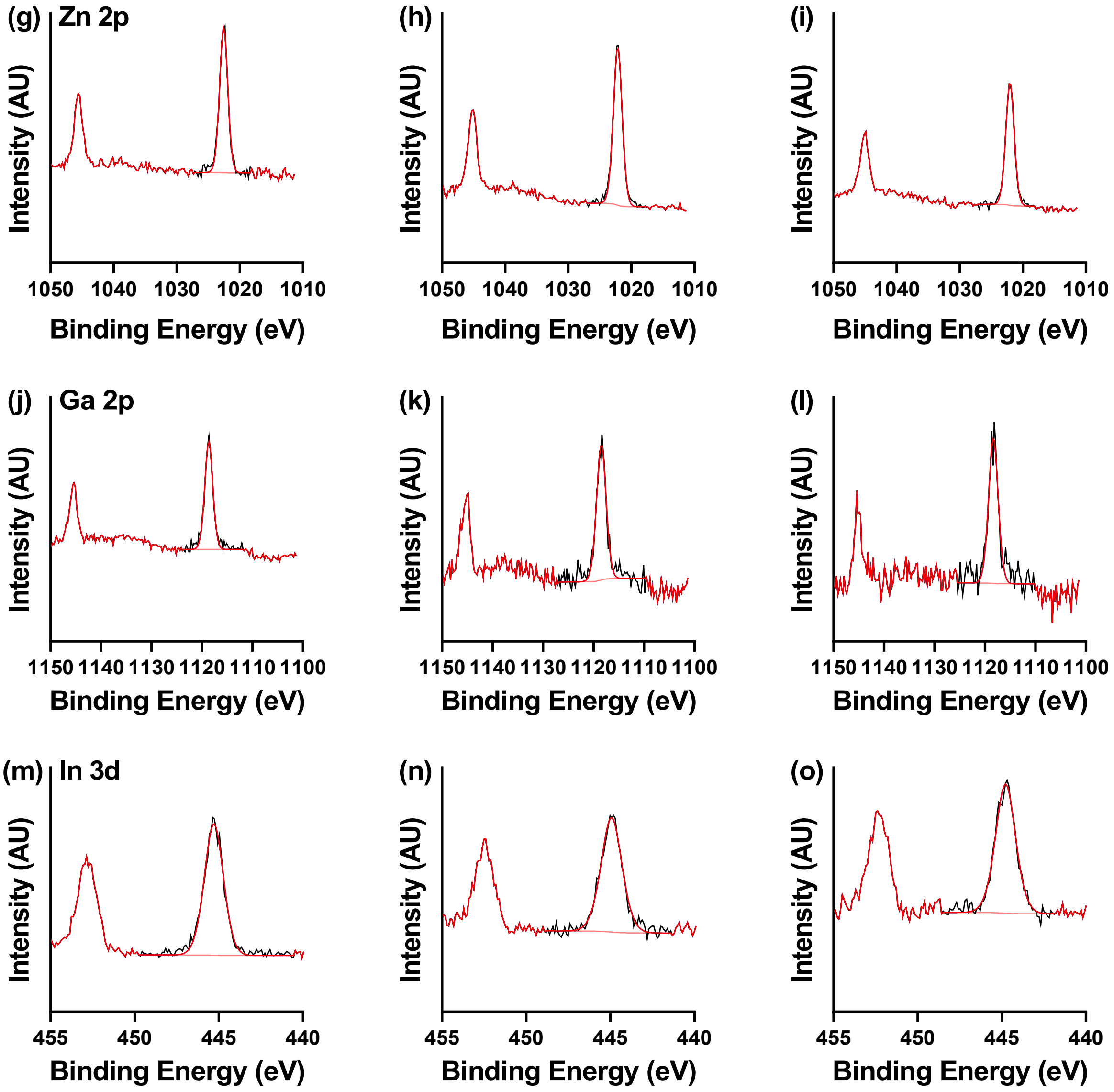

Figure S24. Fitting for metal core levels from HAXPES with (a – c) Co 2p, (d – f) Cu 2p, (g – i) Zn 2p, (j – l) Ga 2p and (m – o) In 3d. The position of the measurement in the film is represented by (a, d, g, j, m) 0 – 4 mm of the film, (b, e, h, k, n) 8 – 12 mm and (c, f, i, l, o) 16 – 20 mm of the film.

Table S9. Table of data from HAXPES atomic% analysis (including C and O).

HAXPES	**Position**		
	1	**5**	**9**
C	12.6	9.4	20
O	11.2	7.4	5.4
Co	0.0	0.0	3.4
Cu	4.3	2.4	4.0
Zn	5.5	8.1	10.6
Ga	9.6	3.6	4.2
In	5.0	2.9	4.6
S	51.9	66.3	47.8

Table S10. Table of data from HAXPES atomic% analysis (excluding C and O).

HAXPES	**Position**		
	1	**5**	**9**
Co	0.0	0.0	4.6
Cu	5.6	2.9	5.4
Zn	7.2	9.7	14.2
Ga	12.6	4.3	5.6
In	6.6	3.5	6.2
S	68.0	79.6	64.1

UV-Vis

UV-Vis was measured, and band gap determined based on the Tauc plot for selective areas of the high entropy metal sulfide thin film. All band gaps were found to be within the 1.8 – 1.9 eV range so the relative change in elemental composition across the film is not found to have a significant impact on the band gap energy of the material.

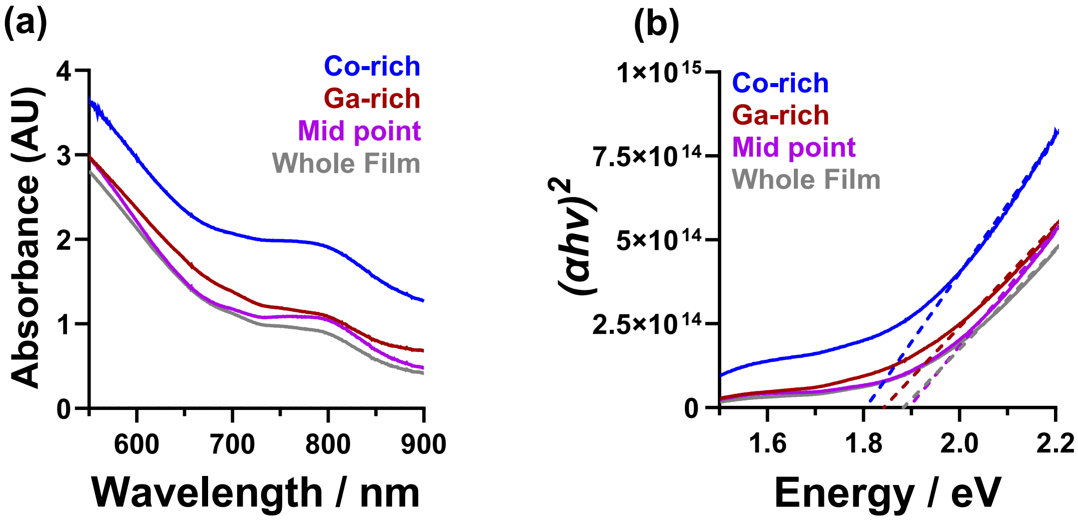

Figure S25. UV absorption spectrum and related Tauc plot.

Table S11. Table of data for band gap energies measured at different parts of the film.

Sample area	E_g / eV
Co-rich (*ca.* position 8)	1.8
Ga-rich (*ca.* position 2)	1.8
Mid-point (*ca.* position 5)	1.8
Whole film	1.9

Cross Sectional SEM images of Film

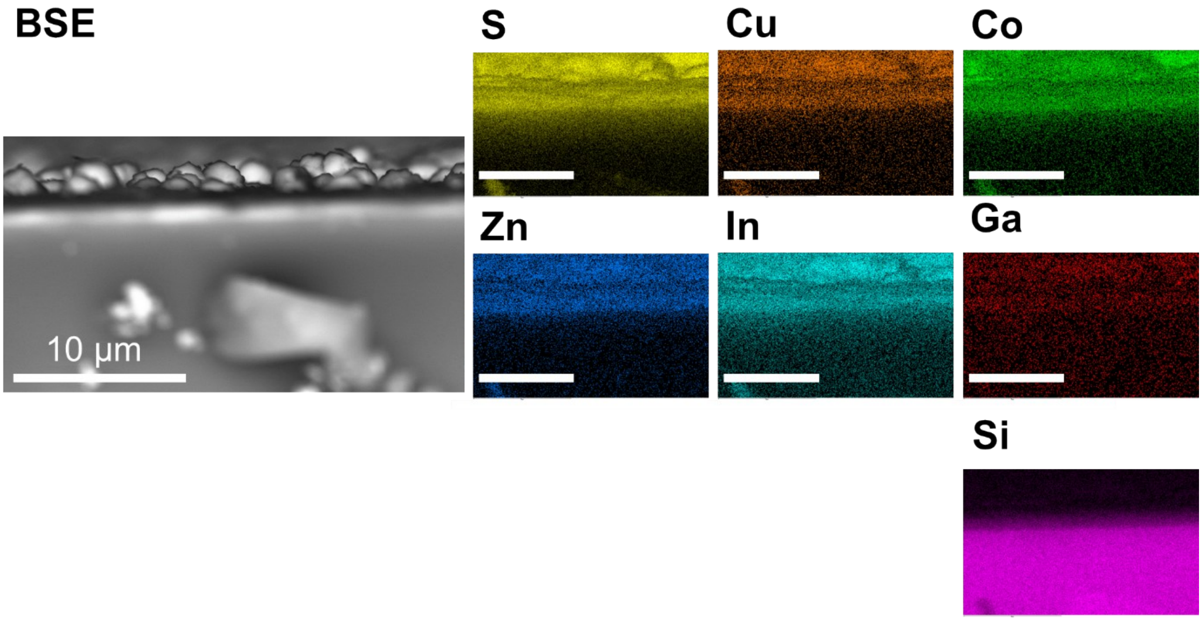

Fig S26 – cross sectional SEM image of HE thin film, with associated EDX spectroscopic mapping.

References

1. J. P. H. Li, X. Zhou, Y. Pang, L. Zhu, E. I. Vovk, L. Cong, A. P. van Bavel, S. Li and Y. Yang, *Phys Chem Chem Phys*, 2019, **21**, 22351-22358.
2. G. Murtaza, S. Alderhami, Y. T. Alharbi, U. Zulfiqar, M. Hossin, A. M. Alanazi, L. Almanqur, E. U. Onche, S. P. Venkateswaran and D. J. Lewis, *ACS Appl Energy Mater*, 2020, **3**, 1952-1961.
3. M. A. Buckingham, B. Ward-O'Brien, W. Xiao, Y. Li, J. Qu and D. J. Lewis, *Chem Commun* , 2022, **58**, 8025-8037.
4. M. A. Buckingham, J. M. Skelton and D. J. Lewis, *Crystal Growth & Design*, 2023, DOI: 10.1021/acs.cgd.3c00712.
5. R. Shannon, *Acta Crystallographica Section A*, 1976, **32**, 751-767.